Published in final edited form as:
Nano Lett. 2007 March ; 7(3): 596–601. doi:10.1021/nl0624723.

Intracellular distribution of TiO_2-DNA oligonucleotide nanoconjugates directed to nucleolus and mitochondria indicates sequence specificity

Tatjana Paunesku[1,2], **Stefan Vogt**[3], **Barry Lai**[3], **Jörg Maser**[3], **Nataša Stojicevic**[1], **Kenneth T. Thurn**[1], **Clodia Osipo**[4], **Hong Liu**[2], **Daniel Legnini**[3], **Zhou Wang**[5], **Chung Lee**[6], and **Gayle E. Woloschak**[1,2,7,8,*]

[1]Department of Radiation Oncology, Northwestern University, Chicago, IL

[2]Robert H. Lurie Comprehensive Cancer Center, Northwestern University, Chicago, IL

[3]X-ray Science Division, Advanced Photon Source, Argonne National Laboratory, Argonne, IL

[4]Cardinal Bernadin Cancer Center, Loyola University Medical Center, Maywood, IL

[5]Department of Urology, University of Pennsylvania Medical Center, Pittsburgh, PA

[6]Department of Urology, Northwestern University, Chicago, IL

[7]Department of Radiology, Northwestern University, Chicago, IL

[8]Department of Cell and Molecular Biology, Northwestern University, Chicago, IL

Abstract

Deoxy DNA oligonucleotides hybridize to matching DNA sequences in cells, as established in the literature, depending on active transcription of the target sequence and local molarity of the oligonucleotide. We investigated the intracellular distribution of nanoconjugates composed of deoxy DNA oligonucleotides attached to TiO_2 nanoparticles, thus creating a locally increased concentration of the oligonucleotide. Two types of nanoconjugates, with oligonucleotides matching mitochondrial or nucleolar DNA, were specifically retained in mitochondria or nucleoli.

The use of free nucleic acids as therapeutic agents was conceptualized at the same time when the first attempts in genetic engineering were successfully concluded. Notwithstanding the difficulties regarding cellular uptake and intracellular stability of nucleic acids, oligonucleotides were found to be capable of "finding" the matching genomic sequence and leading to the repair of the target sequence[1–4]. The formation of matching hybrids inside cells is modulated by processes of transcription and replication.

Our interest lies in using a similar approach in order to develop an agent that can be triggered to cause not genomic DNA repair but the opposite—DNA damage extensive enough to cause gene inactivation. For this purpose we are developing TiO_2 nanoparticles (3–5 nm) conjugated to 1 to 5 single stranded DNA oligonucleotides (6–8 nm) via dopamine used as a bidentate enediol ligand for TiO_2 5. The semiconductor TiO_2 nanoparticles can be excited causing the electropositive holes to be injected into the DNA ultimately leading to DNA scission as we have shown *in vitro* [5, 6].

*to whom reprint requests should be addressed: g-woloschak@northwestern.edu.

The first step in developing nanoparticles for intracellular DNA targeting is to assure that they have the capacity to be taken up by cells and retained at their target DNA sequence. Since it is very difficult to identify the precise position of a single gene DNA target inside cells, we decided to monitor targeting of genes located in specific subcellular compartments. Two such DNA targets with clearly defined subcellular locations are genes for ribosomal RNA (rDNA) located in nucleolus inside cell nucleus; and mitochondrial genes, located in mitochondria in cellular cytoplasm. Therefore, we decided to compare 1) oligonucleotide targeting ribosomal 18S RNA gene (R18) located on the satellite arms of chromosomes and dispersed in the area of nucleolus in the interphase nucleus; 2) oligonucleotide targeting the mitochondrial genomic sequence—NADH dehydrogenase subunit 2 gene (ND2), and 3) nanoparticles without attached oligonucleotide DNA. While the DNA-free nanoparticles have no target inside cells, nucleolar and mitochondrial nanoconjugates have similar number of targets per cell, albeit distributed differently. Ribosomal 18S gene is present in the genome in about 300 hundred copies [7] co-localized in one location—in nucleoli. The mitochondrial target is present in a few copies in each mitochondrion; since the majority of cells have several hundred mitochondria [8] this target sequence has similar frequency as the nucleolar target sequence, yet this target is interspersed throughout the cytoplasm.

For the experiments described here TiO_2-DNA nanoconjugates were prepared fresh as described 5. A colloidal nanoparticle solution with approximately 10 μM nanoparticle concentration was conjugated to dopamine modified oligonucleotides. Nanoconjugates were prepared so that on the surface of each nanoparticle, otherwise covered with glycidyl isopropyl ether, one to five dopamine-modified DNA molecules were attached. Sequences of the oligonucleotides attached to the nanoparticles were: (1) specific for the sense strand sequence of the NADH dehydrogenase 2 (ND2) mitochondrial gene present in the PC12 cell line: 5’ carboxy dT-cacgacaccttagcaccaacttac (ND2s); or (2) matching the sense stand of the R18S ribosomal RNA gene: 5' carboxy dT-ttccttggatgtggt (R18Ss) universally present in mammalian cells. Sense strand oligonucleotides were chosen for these experiments in order to avoid hybridization with the RNA products of the two genes. The nanoparticles are coated with glycidyl isopropyl ether which reduces their surface reactivity with the vast majority of chemical groups, making them non-reactive with most biological molecules. Therefore, oligonucleotide free nanoparticles showed little retention inside cells at the 24 hours post-transfection time-point, while nanoconjugates with oligonucleotides remained inside cells (Figures 1–6).

We transfected human breast cancer cell line MCF-7/WS8 with nanocomposites specific for nucleolar target sequence (Figure 1). The cells were grown according to the instructions recommended by American Type Culture Collection (ATCC) to 80% confluence and at that time serum starved (incubated in serum free medium) for 16 hours. Transfection was done by electroporation: $1–3\times10^6$ cells were electroporated with 5–15 μl of 10 μM nanoconjugate solution (with 2–6 oligonucleotides per particle) using the Mammozapper™ apparatus (Tritech, Carlsbad, CA) following the manufacturer’s instructions. The electroporated cells were resuspended in 8ml of complete medium and allowed to attach to the tissue culture dishes for 2 hours; at that time cells were washed free of excess nanoconjugates: medium was removed, cells were rinsed with the new complete medium, and then 10 ml of the fresh medium was added to cells for an additional 24 hours. At the end of this time cells were harvested for imaging.

Since nanoconjugates can not be visualized by optical microscope, we used two alternative approaches to determine their localization. One technique available to us was transmission electron microscopy. Ultra-thin (100 nm) sections of transfected cells embedded in epoxy resin were cut with a diamond knife onto 200 mesh nickel grids, stained with osmium tetraoxide, uranyl acetate and lead citrate. Analyses of cell sections were performed in a

transmission electron microscope (JEOL 1220, JEOL USA, MA). Imaging was done at Northwestern University Cell Imaging core facility. The density of TiO_2 surpasses the density of cellular material and we were able to determine the presence of TiO_2 in two regions ~0.5 μm inside the nuclei of nanoconjugate treated cells.At the same time no such "denser" material was found in mitochondria of these cells.

A more direct approach to image titanium itself is to detect it by K alpha characteristic X-ray fluorescence using X-ray fluorescence microscopy (XFM). This technique allows simultaneous mapping of chemical elements by their K alpha specific fluorescence. The XFM facility we used at 2-ID-E and 2-ID-D beamlines at the Advanced Photon Source at Argonne National Laboratory is best equipped for mapping of elements between Si and Zn in the periodic table. An undulator source was used to generate hard x-rays with energy of 10 keV. A single bounce Si <111> monochromator was used to monochromatize the X-rays; they were then focused to a beam spot ~0.4x0.3 microns in size using Fresnel zone plate optics with a focal length of 25 cm (Xradia, Concord, CA) at 2-ID-E beamline; or a beam spot ~0.3x0.2 μm is obtained using a Fresnel zone plate with focal length of 12.9 cm is produced at the 2-ID-D beamline. Characteristic X-ray induced X-ray fluorescence was detected using an ultra-LEGe energy dispersive detector (Canberra, Meriden, CT). Elemental maps were built point by point—raster-scanning the sample by moving it through the focal spot. The fluorescence spectra were acquired at every specimen position and were fitted with modified Gaussians corresponding to X-ray fluorescence lines. Quantification was done by comparison of normalized fluorescence counts from the sample to NBS thin film standards 1832 and 1833 (NIST, Gaithersburg, MD). Elemental quantification and co-localization of elemental signals was investigated using MAPS program [9].

The XFM technique is used for imaging of whole cells, which enables one to determine the total elemental content in the complete volume of the desired region of interest. P, Ti and Zn elemental maps were acquired simultaneously; the presence of P and Zn signals indicates the outline of the cells while the "internal" more intense P and Zn signals suggest the area of the nucleus. The pattern of spots indicates the presence of Ti (and therefore nanoconjugates) in the nuclei.

In order to ensure that these results are not unique to MCF-7/WS8 cells we investigated transfection of other cell types: PC3 human prostate cell line (Figure 2) and rat pheochromocytoma cell line PC12 (data not shown). Moreover, we used different approaches for transfection, comparing their results to the results obtained by electroporation. Transfection by electroporation can be considered as a "gold standard" approach because it delivers the transfection material equally in every subcellular compartment. It is therefore retention of nanoconjugates that dictates their localization in cells at 24 hours post transfection. We were able to observe nanoconjugate retention in cells of different origins because we were using the nucleolar nanoconjugate with an universal probe sequence that targets rRNA 18S genes in most mammalian species. Cancer cells most often contain 2 or more nucleoli—in these cells the Ti signal was often found to look like a pair of spots (Figure 1 and 2). XFM elemental maps of prostate cancer PC3 cells (Figure 2), same as breast cancer MCF7/WS8 cells (Figure 1) and pheochromocytoma cells (data not shown) showed in most cases a two-spot pattern. This type of pattern was, moreover, present both in electroporated cells (Figures 1, 2a) and cells that were transfected by nanoconjugates by natural uptake.

To address the capacity of nanoconjugates to be retained inside mitochondria we used a mitochondrial nanoconjugate specific for NADH dehydrogenase 2 to transfect rat pheochromocytoma cell line PC12 by electroporation (Figures 3 and 4) or natural uptake (Figure 5).

PC12 cells electroporated by mitochondria specific nanoconjugate were imaged both by XFM mapping and by transmission electron microscopy (Figure 3). In the TEM images of these cells we found no granular material in the nuclei. Mitochondria, on the other hand contained denser granular material resembling the nanoparticles.

In addition to imaging of whole cells and cell sections, we used electroporated PC12 cells as a source from which we have isolated free mitochondria. In this case sectioning of the cell was not necessary to show the presence of nanoconjugates inside mitochondria. Isolated mitohondria were imaged by XFM (Figure 4), showing presence of titanium.

Elemental maps of P, S, Cl, K, Ca, Ti, Mn, Fe, Cu, Zn were done for mitochondria isolated from PC12 cells electroporated with nanoconjugates carrying ND2s oligonucleotide and then “washed” for 24 hours in nanoconjugate free medium. Elemental maps show the range of concentrations in the sample in a “red temperature scale” from highest (white) to lowest signal (black). The scan area was 3x3 μm, with a step size of 0.1 μm. Scanning was done at 2ID-D beamline at the APS. Elemental concentrations are shown in micrograms per cm^2. Size bar is 1 micron.

In addition to electroporation we transfected PC12 cells with mitochondria specific nanoconjugates by natural uptake. We could not test the retention of this nanoconjugate in any other cell type since oligonucleotides probe—ND2s oligonucleotide matches only the rat mitochondrial genomic sequence. Following a 24 wash, we imaged PC12 cells transfected by mitochondrial nanoconjugate by XFM (Figure 5a). A detailed image of the region likely containing a mitochondrion is shown in Figure 5b. The more intense Mn signal outlines the mitochondria in Figure 5b due to the increased presence of this metal in the mitochondrial matrix, bound to mitochondrial manganese superoxide dismutase protein.

Figure 6 shows a correlation between the specific types of the nanoconjugates used—free TiO_2 nanoparticle (without DNA attached), nucleolar nanoconjugate and mitochondrial nanoconjugate and ratio of Ti to Zn in these cells. We used cluster analysis to define cells as regions of interest, calculated elemental content for these P, S, Ca, Zn and Ti within the cells and calculated, for P, S, Ca, and Ti, the average normalized elemental content using Zn quantity for normalization. Zn is present in all cells, co-localized with cellular material and therefore completely overlaps with other natural cellular elements such as P, S, and Ca. Because of that, ratios of the elemental concentrations of P/Zn, S/Zn and Ca/Zn were the same in all three groups of samples. However, the variation between the ratios of Ti/Zn between the three groups of cells transfected with three types of nanoconjugates was statistically significant (Figure 6, Supplemental Table 1). This statistical analysis was done using GraphPad InStat3 software version 3.06 (GraphPad, San Diego, California). A nonparametric ANOVA test—Kruskal-Wallis Statistic was used; Dunn’s Multiple Comparison Test was used to evaluate probability of statistical significance of mean ranks difference between samples.

In conclusion, in our experiments different nanoconjugates were retained in detectable quantity only in those subcellular compartments for which the nanoconjugates were designed: nucleolar nanoconjugates inside nuclei and mitochondrial nanoconjugates in mitochondria. In each experiment the absence of the tested nanoconjugate from the non-targeted subcellular compartment served as a negative control. Mitochondrial and nucleolar nanoconjugates differed only in the nucleotide sequence of their DNA oligonucleotides, and no other aspect of the nanoconjugate synthesis: the nanoparticles came from the same pool of nanoparticles, both oligonucleotides were attached to the dopamine at the same time and using the same technique and subsequently mixed with the nanoparticles in order to create the final nanoconjugates. Therefore, sequence-specific retention of the nanoconjugates is

based on the ability of the oligonucleotide component of the nanoconjugate to establish DNA hybrid with the complementary intracellular sequence. The high rate of transcription in both mitochondria and nucleoli is probably one of the deciding factors that made these results possible.

The uptake of nanoconjugates by all three methods tested resulted in presence of nanoconjugates inside cells; therefore it appears that the TiO_2 bound oligonucleotides behave similarly to oligonucleotides alone. Natural uptake of DNA can be either enocytosis or receptor mediated, depending on the concentration of DNA [10]. In both cases a certain amount of transfected DNA does end up inside the nucleus. Uptake of DNA by mitochondria was also detected in those experiments where electroporation was used as a means for transfection [11].

The number and uses of bio-nanoconjugates are growing daily. Medical imaging techniques (encompassing detection, identification and diagnostics), therapeutics and basic science are all beginning to benefit from the use of nanoscale materials—such as metal and metal oxide nanoparticles, nanowires and quantum dots [12, 13, 14, 15, 16, 17] reaching such new grounds as *in vivo* imaging [18, 19], delivery of drug payloads [12, 14] and have long begun to improve photodynamic and heat therapy [20, 21].

Nanoconjugates with oligonucleotide components exist in several guises—with nanoparticles made of different materials [5, 12, 13, 15, 16, 22]. Functions of these nanoconjugates are varied as well—from imaging [17, 18, 21] to nucleic acid, DNA [5] or RNA [13] hybridization and/or cleavage, with or without aid from the cellular enzymatic machinery. In this work we determined sequence specificity of the subcellular retention of TiO_2-DNA nanoconjugates, suggesting that it is possible to use the TiO_2-DNA nanoconjugates for sequence specific local treatment of DNA targets.

Supplementary Material

Refer to Web version on PubMed Central for supplementary material.

Acknowledgments

This work was supported by NIH CA107467, EB002100, P50 CA89018, U54CA119341 and by DOE FG02-04 ER 63920. TiO_2 nanoparticles used for some of these studies were a gift from T. Rajh and M. Thurnauer (Chemistry Division, Argonne National Laboratory, Argonne, IL). TEM was done at Northwestern University Cell Imaging Facility and we are grateful to Lennell Reynolds for his help with sample preparation and TEM imaging. XFM experiments were performed at 2ID-E and D beamlines of the X-ray Operations and Research, Advanced Photon Source, Argonne National Laboratory. Use of the Advanced Photon Source was supported by the U. S. Department of Energy, Office of Science, Office of Basic Energy Sciences, under Contract No. W-31-109-Eng-38.

References

1. Kren BT, et al. Modification of hepatic genomic DNA using RNA/DNA oligonucleotides. Gene Ther. 2002; 9:686–690. [PubMed: 12032688]
2. Andersen MS, Sorensen CB, Bolund L, Jensen TG. Mechanisms underlying targeted gene correction using chimeric RNA/DNA and single-stranded DNA oligonucleotides. J Mol Med. 2002; 80:770–781. [PubMed: 12483462]
3. Igoucheva O, Alexeev V, Yoon K. Targeted gene correction by small single-stranded oligonucleotides in mammalian cells. Gene Ther. 2001; 8:391–399. [PubMed: 11313816]
4. Liu L, Rice MC, Kmiec EB. In vivo gene repair of point and frameshift mutations directed by chimeric RNA/DNA oligonucleotides and modified single-stranded oligonucleotides. Nucleic Acids Res. 2001; 29:4238–4250. [PubMed: 11600713]

5. Paunesku T, et al. Biology of TiO2-oligonucleotide nanocomposites. Nature Materials. 2003; 2:343–346.
6. Paunesku T, et al. Intracellular localization of titanium dioxide-biomolecule nanocomposites. Journal De Physique Iv. 2003; 104:317–319.
7. Makalowski W. The human genome structure and organization. Acta Biochim Pol. 2001; 48:587–598. [PubMed: 11833767]
8. Allard C, De Lamirande G, Cantero A. Mitochondrial population of mammalian cells. II. Variation in the mitochondrial population of the average rat liver cell during regeneration; use of the mitochondrion as a unit of measurement. Cancer Res. 1952; 12:580–583. [PubMed: 14945049]
9. Vogt S, Maser J, Jacobsen C. Data analysis for X-ray fluorescence imaging. Journal De Physique Iv. 2003; 104:617–622.
10. de Diesbach P, et al. Receptor-mediated endocytosis of phosphodiester oligonucleotides in the HepG2 cell line: evidence for non-conventional intracellular trafficking. Nucleic Acids Res. 2002; 30:1512–1521. [PubMed: 11917011]
11. McGregor A, Temperley R, Chrzanowska-Lightowlers ZM, Lightowlers RN. Absence of expression from RNA internalised into electroporated mammalian mitochondria. Mol Genet Genomics. 2001; 265:721–729. [PubMed: 11459193]
12. Ferrari M. Nanovector therapeutics. Curr Opin Chem Biol. 2005; 9:343–346. [PubMed: 15967706]
13. Rosi NL, et al. Oligonucleotide-modified gold nanoparticles for intracellular gene regulation. Science. 2006; 312:1027–1030. [PubMed: 16709779]
14. Ferrari M. Cancer nanotechnology: opportunities and challenges. Nat Rev Cancer. 2005; 5:161–171. [PubMed: 15738981]
15. Bruchez M Jr, Moronne M, Gin P, Weiss S, Alivisatos AP. Semiconductor nanocrystals as fluorescent biological labels. Science. 1998; 281:2013–2016. [PubMed: 9748157]
16. Cao YC, Jin R, Mirkin CA. Nanoparticles with Raman spectroscopic fingerprints for DNA and RNA detection. Science. 2002; 297:1536–1540. [PubMed: 12202825]
17. Park SJ, Taton TA, Mirkin CA. Array-based electrical detection of DNA with nanoparticle probes. Science. 2002; 295:1503–1506. [PubMed: 11859188]
18. Winter PM, et al. Molecular imaging of angiogenesis in nascent Vx-2 rabbit tumors using a novel alpha(nu)beta3-targeted nanoparticle and 1.5 tesla magnetic resonance imaging. Cancer Res. 2003; 63:5838–5843. [PubMed: 14522907]
19. Smith AM, Gao X, Nie S. Quantum dot nanocrystals for in vivo molecular and cellular imaging. Photochem Photobiol. 2004; 80:377–385. [PubMed: 15623319]
20. Allemann E, et al. Photodynamic therapy of tumours with hexadecafluoro zinc phthalocynine formulated in PEG-coated poly(lactic acid) nanoparticles. Int J Cancer. 1996; 66:821–824. [PubMed: 8647656]
21. Ito A, Shinkai M, Honda H, Kobayashi T. Heat-inducible TNF-alpha gene therapy combined with hyperthermia using magnetic nanoparticles as a novel tumor-targeted therapy. Cancer Gene Ther. 2001; 8:649–654. [PubMed: 11593333]
22. Fu AH, et al. Discrete nanostructures of quantum dots/Au with DNA. J Am Chem Soc. 2004; 126:10832–10833. [PubMed: 15339154]

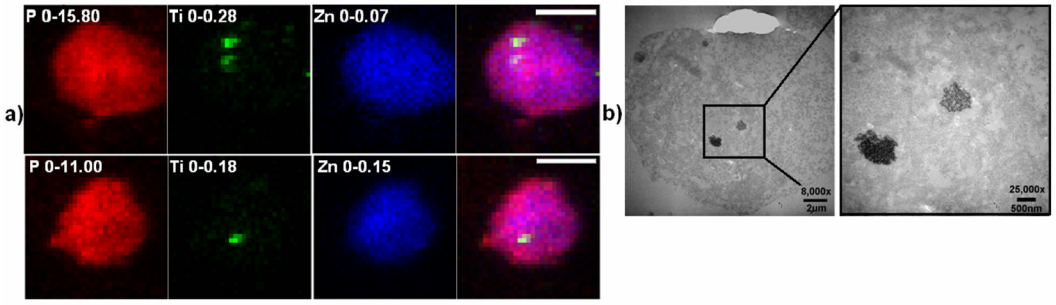

Figure 1. XFM maps and TM images of MCF7/WS8 cells transfected with nucleolus specific nanoconjugates

a) MCF7/WS8 cells were electroporated and imaged by X-ray fluorescence microscopy. Elemental maps and map overlaps are shown for P, Ti, and Zn. Scanning was done at 2ID-E beamline at the APS. White size bars are 10 microns. Numbers following elemental sign show elemental concentration in micrograms per cm^2.

b) TEM image of 100 nm thin section of a MCF7/WS8 cells electroporated with nucleolus specific nanoconjugate; left panel: cell cross section; right panel: TEM detail with two nanoconjugate rich spots. Imaging was done at Northwestern University Cell Imaging core facility.

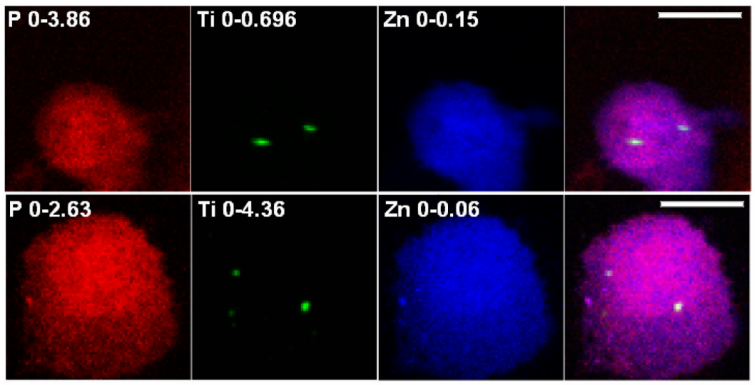

Figure 2. XFM maps of whole PC3 cells transfected with nucleolus specific nanoconjugates
Top row: electroporation; bottom row: natural uptake. In both cases elemental maps and map overlaps are shown for P, Ti, and Zn. Scanning was done at 2ID-E beamline at the APS. White size bars are 10 microns. Numbers following elemental sign show elemental concentration in micrograms per cm^2.

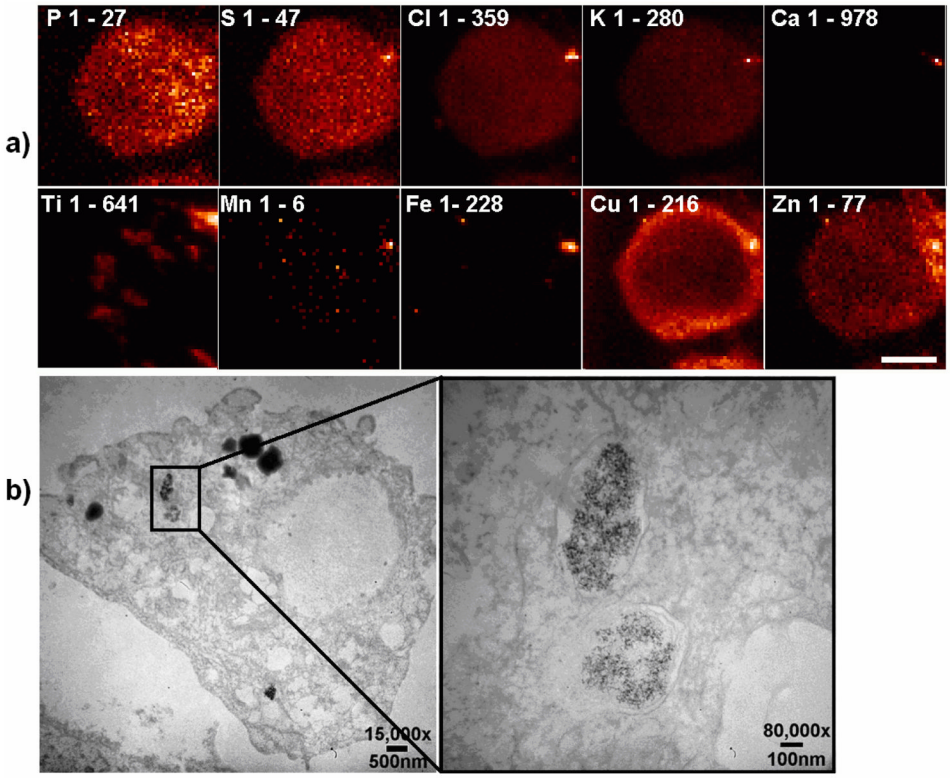

Figure 3. XFM and TEM images of PC12 cells electroporated with mitochondria specific TiO_2-DNA nanoconjugates

a) XFM maps for P, S, Cl, K, Ca, Ti, Mn, Fe, Cu and Zn of a whole PC12 cell electroporated by a mitochondria specific nanoconjugate. Elements are indicated inside each map. Elemental concentrations are given as relative signal intensity. Size bar is 5 micron. b) TEM image of a 100 nm thin section of a PC12 cell electroporated by a mitochondria specific nanoconjugate. Left—cell with several mitochondria containing nanoconjugate. Right—detailed image of two adjacent mitochondria. The very dense non-granular material located in the cell vacuoles is osmium tetraoxide.

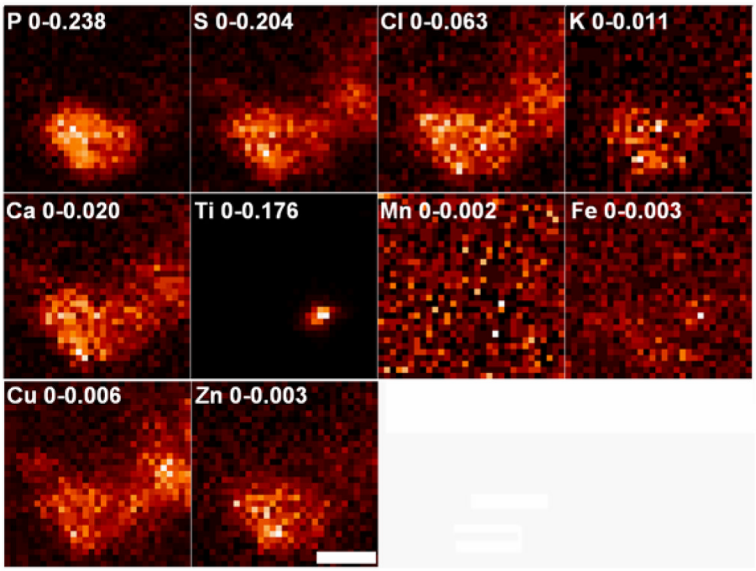

Figure 4.
XFM map of isolated mitochondria of PC12 cells electroporated with mitochondria specific (NADH dehydrogenase 2 specific) nanoconjugates.

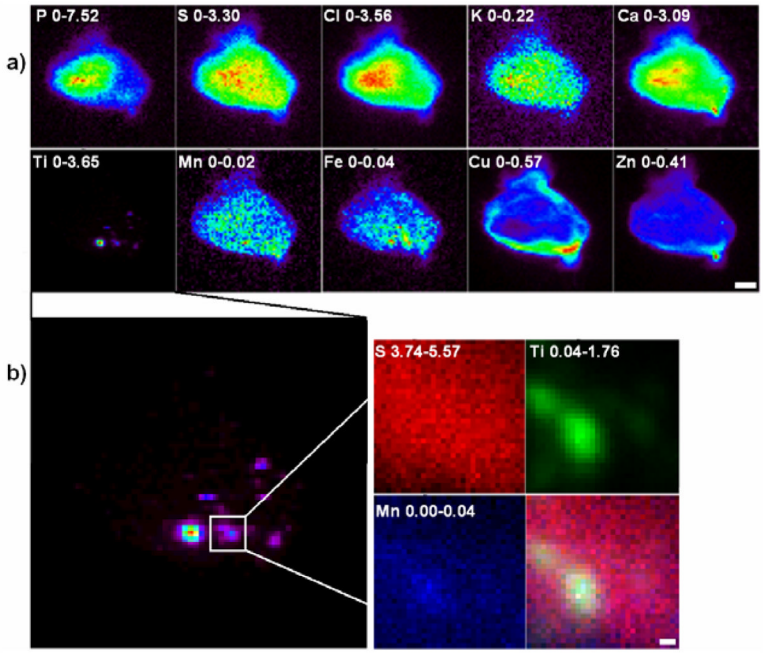

Figure 5. XFM maps of whole PC12 cell transfected with mitochondria-specific nanoconjugates using natural uptake

a) Elemental maps of P, S, Cl, K, Ca, Ti, Mn, Fe, Cu, Zn in PC12 cell treated with nanoconjugates carrying ND2s oligonucleotide for 24 hours and then "washed" for 24 hours in nanoconjugate free medium. Elemental maps show the range of concentrations in the sample in a rainbow color scale from highest (red) to lowest signal (black). Scan area was for the cell on the left 32x32 micron, 0.3 micron step; for the cell on the right 13x12.8 micron, 0.2 micron step. Scanning was done at 2ID-D beamline at the APS. Elemental concentrations are given in micrograms per cm^2. White size bar is 2 microns.

b) Enlarged Ti maps of the cells in a) and a detailed XFM map of a mitochondria inside the cell. Left—enlarged Ti map of the whole cell from the right panel of Figure 3a. Right—S, Ti, Mn and overlap maps for the mitochondria shaped form from the left panel. The scan area was 1.5x1.5 micron with 50 nm step. Scanning was done at 2ID-D beamline at the APS. White size bar is 10 nanometers.

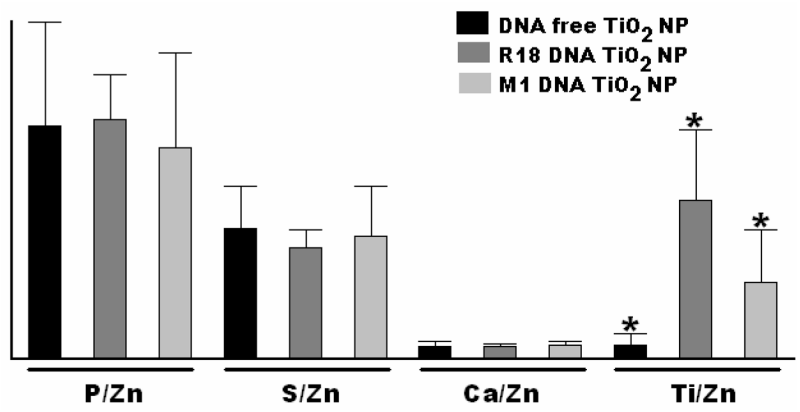

Figure 6.

Ratios of intracellular concentrations of P, S, Ca and Ti compared to Zn when different nanoparticles/nanoconjugates are used. Each type of nanoparticle/ nanoconjugate transfection was indicated by different colors: DNA-free TiO_2 nanoparticles (DNA free TiO_2 NP) black, nanoconjugates specific for nucleolar rDNA (R18 DNA TiO_2 NP) dark grey, and nanoconjugates specific for mitochondrial DNA (M1 DNA TiO_2 NP) light grey. Elemental ratios for each group of three sample preparations were shown together as indicated below the graph. Average ratios were derived from several scans (15 for free nanoparticle, 7 for ribosomal rDNA, and 9 for mitochondrial DNA) and shown as bar graphics, with the standard deviation shown as overlaid error bars. Samples showing statistically significant variation are indicated by asterisks.